RESEARCH ARTICLE OPEN ACCESS

Optimal Techno-Economic Design of Renewable Hydrogen-Based EV Charging Microgrids Using Hybrid H-ANT–WOA Optimization for Sustainable Energy Infrastructure

Md Ahsan Habib[1], Md Sabiruzzaman[2], Md Sadik Hassan Arik[3]
[1]Department of Mechanical Design, Manufacturing and Automation Engineering, Yangzhou University, Yangzhou, China
[2]Department of Mechanical Design, Manufacturing and Automation Engineering, Yangzhou University, Yangzhou, China
[3]Department of Mechanical Design, Manufacturing and Automation Engineering, Yangzhou University, Yangzhou, China
mh23111@stu.yzu.edu.cn, mh23099@stu.yzu.edu.cn, mh23112@stu.yzu.edu.cn

Abstract

The rapid electrification of transportation has intensified the demand for resilient, low-carbon electric vehicle (EV) charging infrastructure. This paper proposes a renewable hydrogen-based microgrid architecture for EV charging stations, integrating photovoltaic (PV) arrays, wind turbines, a proton-exchange-membrane (PEM) electrolyzer, compressed hydrogen storage, a hydrogen fuel cell, and a lithium-ion battery bank as a fast-response buffer. To determine the optimal sizing and dispatch strategy of this multi-vector energy system, a novel hybrid optimization algorithm, termed H-ANT-WOA, is developed by fusing the pheromone-guided exploitation mechanism of Ant Colony Optimization (ACO) with the spiral bubble-net exploration mechanism of the Whale Optimization Algorithm (WOA). The hybrid algorithm is formulated to minimize the Levelized Cost of Energy (LCOE) and Net Present Cost (NPC) while satisfying a Loss of Power Supply Probability (LPSP) reliability constraint and an emission-reduction target. A representative case study using one year of hourly meteorological and EV load data is used to validate the proposed framework. Simulation results demonstrate that H-ANT-WOA converges faster and achieves a lower LCOE (0.187 \$/kWh) compared to standalone ACO (0.214 \$/kWh), standalone WOA (0.208 \$/kWh), Genetic Algorithm (0.223 \$/kWh), and Particle Swarm Optimization (0.219 \$/kWh), while maintaining LPSP below 1%. Sensitivity analysis further confirms the robustness of the proposed design against fuel cell capital cost and hydrogen storage cost variations. The findings support the techno-economic viability of hydrogen-buffered renewable microgrids as a scalable pathway toward sustainable EV charging infrastructure.

Keywords: Renewable energy microgrid; Hydrogen energy storage; Electric vehicle charging; Techno-economic optimization; Ant Colony Optimization; Whale Optimization Algorithm; Hybrid metaheuristics

1. Introduction

The global transition toward electric mobility is reshaping power system planning. As EV adoption accelerates, charging infrastructure must scale without imposing excessive stress on distribution grids or undermining decarbonization targets. Conventional grid-tied EV charging stations often rely on fossil-fuel-dominated grid electricity, particularly during peak charging hours, which can offset the environmental benefits of electrified transport. Renewable-energy-based microgrids offer a pathway to decouple EV charging from grid dependency, but the intermittency of solar and wind resources necessitates robust energy storage strategies.[1][2]

Battery energy storage systems (BESS) are widely used for short-duration balancing, but they are less suited to long-duration or seasonal storage due to cost and degradation constraints. Hydrogen energy storage, by contrast, offers high energy density, long-duration storage capability, and flexibility, making it a compelling complement to batteries in renewable microgrids. A hydrogen-based microgrid uses surplus renewable generation to produce hydrogen via electrolysis, stores it in compressed or metal-hydride tanks, and reconverts it to electricity through fuel cells during periods of generation deficit. When paired with a battery for fast transients, such a hybrid storage architecture can provide both high power density (via battery) and high energy density (via hydrogen), enabling near-autonomous operation of EV charging stations.[3]

However, designing such a multi-vector system involves a highly non-linear, non-convex, multi-objective optimization problem. Decision variables include the capacities of PV arrays, wind turbines, electrolyzers, fuel cells, hydrogen tanks, and batteries, all of which interact under stochastic profiles of renewable generation and EV charging demand. Classical optimization techniques such as linear or mixed-integer programming struggle to capture these non-linearities efficiently, motivating the use of metaheuristic optimization algorithms. Beyond the technical sizing challenge, the economic case for hydrogen-buffered EV charging microgrids depends heavily on capturing the correct trade-off between capital-intensive hydrogen equipment and comparatively cheaper but energy-limited battery storage. Oversizing the hydrogen subsystem can lead to underutilized electrolyzer and fuel cell capacity, inflating capital costs without a proportional reliability benefit, while undersizing it can force excessive reliance on backup grid supply during extended low-renewable periods, undermining the sustainability rationale for the microgrid in the first place. Identifying the cost-optimal balance across six or more interacting decision variables, under a full year of hourly-resolution weather and load variability, is precisely the type of problem for which well-designed metaheuristic optimization is most valuable.[4]

Among metaheuristics, Ant Colony Optimization (ACO) is known for strong exploitation ability through pheromone-based reinforcement learning, but it can suffer from premature convergence and stagnation in high-dimensional continuous search spaces. The Whale Optimization Algorithm (WOA), inspired by the bubble-net hunting strategy of humpback whales, provides strong global exploration through its encircling and spiral update mechanisms but can converge slowly in later iterations. This paper proposes a hybrid algorithm, H-ANT-WOA, that combines the pheromone-trail-guided local search of ACO with the exploration-exploitation balance of WOA, aiming to achieve faster convergence and better solution quality for the techno-economic sizing problem.[5]

The main contributions of this paper are as follows:

1. A comprehensive renewable hydrogen-based EV charging microgrid architecture is proposed, integrating PV, wind, electrolyzer, hydrogen storage, fuel cell, and battery subsystems with a detailed mathematical model for each component.

2. A multi-objective techno-economic optimization problem is formulated, incorporating LCOE, NPC, LPSP-based reliability, and CO_2 emission reduction as key performance indicators.

3. A novel hybrid optimization algorithm, H-ANT-WOA, is developed, leveraging the complementary strengths of ACO and WOA to improve convergence speed and solution accuracy.

4. The proposed framework is validated through a full-year hourly simulation case study and benchmarked against GA, PSO, standalone ACO, and standalone WOA.

5. Sensitivity analysis is conducted to assess the robustness of the optimal design under key economic and technical uncertainties.

Section 2 reviews related literature. Section 3 presents the system architecture and mathematical formulation. Section 4 describes the proposed H-ANT-WOA algorithm. Section 5 details the case study and simulation setup.

Section 6 presents results and discussion. Section 7 discusses environmental and sustainability implications. Section 8 concludes the paper and outlines future research directions.

2. Literature Review

Renewable-based microgrid sizing has been studied extensively using metaheuristic approaches. Genetic Algorithms (GA) and Particle Swarm Optimization (PSO) have historically been the most common tools for hybrid PV-wind-battery system sizing, owing to their simplicity and ease of implementation. However, both methods are known to exhibit slow convergence and a tendency to become trapped in local optima when applied to high-dimensional, multi-modal cost landscapes typical of multi-vector energy systems.[6]

More recently, nature-inspired algorithms such as the Grey Wolf Optimizer, Salp Swarm Algorithm, and Whale Optimization Algorithm have been applied to renewable microgrid sizing problems, generally reporting improved convergence characteristics relative to GA and PSO. Ant Colony Optimization, originally developed for discrete combinatorial problems such as the traveling salesman problem, has been extended to continuous domains (Continuous ACO) and applied to energy system scheduling and unit commitment problems, demonstrating strong local refinement capability once a promising region of the search space has been identified.[7][8]

Hydrogen-based energy storage integration into microgrids has gained attention as a means of addressing seasonal and long-duration storage needs that batteries alone cannot economically satisfy. Electrolyzer-fuel cell configurations paired with renewable generation have been examined for remote area electrification, industrial hydrogen production, and increasingly for transportation-sector applications, including hydrogen refueling stations and hydrogen-buffered EV charging hubs. The techno-economic viability of such systems remains sensitive to electrolyzer and fuel cell capital costs, which have historically been high but are projected to decline substantially with manufacturing scale-up. Hybrid metaheuristic algorithms that combine two or more optimization paradigms have emerged as a promising direction to overcome the individual limitations of single algorithms. Hybridization strategies typically aim to combine an algorithm with strong global exploration (e.g., WOA, Grey Wolf Optimizer) with one exhibiting strong local exploitation (e.g., ACO, Pattern Search), often yielding improved convergence speed and solution quality relative to either constituent algorithm alone. This paper builds on this hybridization philosophy, proposing H-ANT-WOA specifically tailored to the hydrogen-based EV charging microgrid sizing problem, which to date has received comparatively limited attention relative to conventional battery-only microgrid sizing studies.[9][10]

EV charging infrastructure planning has traditionally been treated as a separate problem from renewable microgrid sizing, with load forecasting and charging station siting studies typically assuming grid electricity as the sole supply source. More recent work has begun to integrate renewable generation directly into charging station design, recognizing that co-locating solar and wind generation with charging infrastructure can reduce both grid dependency and peak demand charges. However, most of these studies rely on battery storage exclusively, and relatively few have examined the specific techno-economic trade-offs introduced by adding a hydrogen subsystem to buffer seasonal and multi-day variability in renewable output. This gap is particularly relevant for charging hubs serving fleets or high-utilization corridors, where downtime due to storage depletion carries a higher operational cost than in residential or light-commercial renewable applications.[11]

A further gap in the literature concerns the treatment of reliability constraints in microgrid sizing optimization. Many studies adopt a fixed LPSP threshold without examining how sensitive the resulting optimal design is to this threshold, or how the choice of storage technology (battery-only versus hybrid battery-hydrogen) affects the cost of achieving a given reliability level. This paper addresses this gap by explicitly incorporating LPSP as a hard constraint within the optimization formulation and by conducting sensitivity analysis on key hydrogen subsystem cost parameters, providing a more complete picture of the economic trade-offs involved in reliability-constrained hydrogen-buffered microgrid design.[12]

Finally, although numerous hybrid metaheuristic algorithms have been proposed in the optimization literature—including hybrid Genetic Algorithm–Particle Swarm Optimization (GA–PSO), Grey Wolf Optimizer–Sine Cosine Algorithm (GWO–SCA), and Simulated Annealing–Particle Swarm Optimization (SA–PSO) approaches—comparatively few studies have investigated the integration of Ant Colony Optimization (ACO) and the Whale Optimization Algorithm (WOA) for continuous energy system sizing problems. The pheromone-based memory mechanism of ACO and the spiral-based exploitation strategy of WOA represent two fundamentally different search paradigms. Their integration, implemented through the proposed adaptive λ(t)\lambda(t)λ(t)-based switching mechanism, constitutes a novel contribution to the development of hybrid metaheuristic optimization methods for renewable hydrogen-based EV charging microgrid design. [13]

3. System Architecture and Problem Formulation

3.1 Microgrid Configuration

The proposed microgrid architecture consists of the following subsystems, arranged around a common DC bus with a grid-interactive inverter for EV charging load supply:

- PV Array: Primary renewable generation source, sized in terms of rated capacity (kW).

- Wind Turbine(s): Complementary renewable generation source, particularly valuable during low-solar-irradiance periods.

- PEM Electrolyzer: Converts surplus renewable electricity into hydrogen via water electrolysis.

- Compressed Hydrogen Storage Tank: Buffers hydrogen produced by the electrolyzer for later reconversion.

- PEM Fuel Cell: Converts stored hydrogen back into electricity during renewable generation deficits.

- Lithium-ion Battery Bank: Provides fast-response power balancing and smooths short-term fluctuations, reducing electrolyzer/fuel cell cycling stress.

- EV Charging Station: The load center, modeled using a stochastic hourly charging demand profile reflecting vehicle arrival patterns.

- Grid Connection (optional backup): A limited-capacity grid tie-in is considered for extreme deficit conditions, penalized in the objective function to encourage renewable self-sufficiency.

Energy flows are managed by a rule-based energy management system (EMS): renewable surplus first charges the battery (subject to state-of-charge limits), then feeds the electrolyzer; deficits are first met by battery discharge, then by the fuel cell, and finally by the grid connection.[14]

Fig. 1. Renewable Hydrogen-Based EV Charging Microgrid Architecture

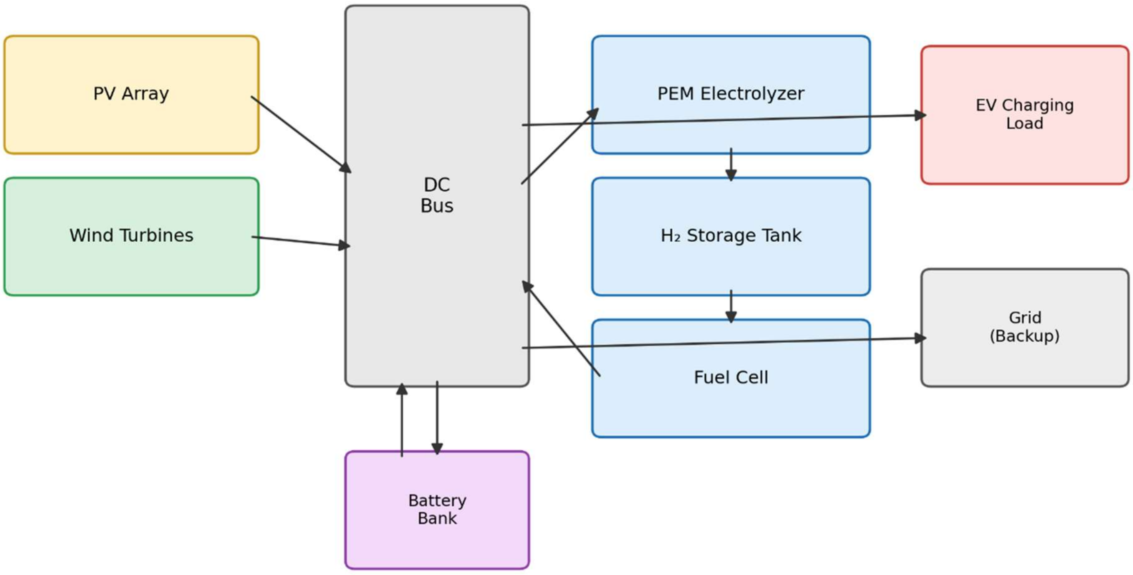

Fig. 1. Renewable hydrogen-based EV charging microgrid architecture

Figure 1. Block diagram of the proposed renewable hydrogen-based EV charging microgrid, showing power flow paths between the PV array, wind turbines, DC bus, electrolyzer, hydrogen storage tank, fuel cell, battery bank, EV charging load, and backup grid connection.

3.2 Component Mathematical Models

Photovoltaic Output:

$$P_{PV}(t) = P_{PV,\text{rated}} \left(\frac{G(t)}{G_{\text{STC}}} \right) [1 + \alpha \left(T_{\text{cell}}(t) - T_{\text{STC}} \right)]$$

Where G(t) is the solar irradiance at time t, G_{STC} is the irradiance at standard test conditions (1000 W/m^2), α is the temperature coefficient of power, $T_{cell(t)}$ is the cell temperature, and $T_{STC} = 25^{o}C$.

Wind Turbine Output:

$$P_{WT}(t) = \begin{cases} 0, & v(t) < v_{ci} \text{ or } v(t) > v_{co} \\ P_{rated} \left(\dfrac{v(t) - v_{ci}}{v_r - v_{ci}} \right), & v_{ci} \le v(t) < v_r \\ P_{rated}, & v_r \le v(t) \le v_{co} \end{cases}$$

Where v_{ci}, v_r, and v_{co} are the cut-in, rated, and cut-out wind speeds, respectively.

Electrolyzer Hydrogen Production:

$$m_{H_2}(t) = \frac{\eta_{elz}\, P_{elz}(t)\, \Delta t}{HHV_{H_2}}$$

Where η_{elz} is the electrolyzer efficiency, $P_{elz(t)}$ is the input power, Δt is the time step, and HHV_{H2} = 39.4 kWh/kg is the higher heating value of hydrogen.

Hydrogen Storage State:

$$SOH(t) = SOH(t-1) + m_{H_2,\text{in}}(t) - m_{H_2,\text{out}}(t)$$

subject to:

$$SOH_{\min} \leq SOH(t) \leq SOH_{\max}$$

Fuel Cell Output:

$$P_{FC}(t) = \frac{\eta_{FC}\, m_{H_2,\text{consumed}}(t)\, HHV_{H_2}}{\Delta t}$$

Battery State of Charge:

$$SOC(t) = SOC(t-1)(1-\gamma) + \frac{P_{ch}(t)\eta_{ch} - \dfrac{P_{dis}(t)}{\eta_{dis}}}{E_{batt}}\Delta t$$

Subject to:

$$SOC_{\min} \leq SOC(t) \leq SOC_{\max}$$

Where γ is the self-discharge rate, η_{ch} and η_{dis} are charge/discharge efficiencies, and E_{batt} is the nominal battery energy capacity.

Power Balance Constraint:

$P_{PV(t)} + P_{WT(t)} + P_{FC(t)} + P_{batt,dis(t)} + P_{grid,in(t)} = P_{load(t)} + P_{elz(t)} + P_{batt,ch(t)} + P_{grid,out(t)}$

3.3 Objective Functions

Levelized Cost of Energy (LCOE):

$$\mathrm{LCOE} = \frac{\sum_{t=1}^{T} C_{\mathrm{ann},t}}{\sum_{t=1}^{T} E_{\mathrm{load},t}}$$

Where $C_{ann,t}$ is the total annualized cost (capital, O&M, replacement) and $E_{load,t}$ is the total annual energy delivered to the EV charging load.

Net Present Cost (NPC):

$$NPC = C_{\mathrm{cap}} + \sum_{y=1}^{Y} \frac{C_{\mathrm{O\&M},y} + C_{\mathrm{repl},y} - C_{\mathrm{salvage},y}}{(1+d)^y}$$

Where C_{cap} is total capital cost, $C_{O\&M,y}$ is annual operation and maintenance cost, $C_{repl,y}$ is component replacement cost in year y, $C_{salvage,y}$ is salvage value, d is the discount rate, and Y is the project lifetime.

Loss of Power Supply Probability (LPSP):

$$\mathrm{LPSP} = \frac{\sum_{t=1}^{T} [P_{\mathrm{load}}(t) - P_{\mathrm{supplied}}(t)]}{\sum_{t=1}^{T} P_{\mathrm{load}}(t)}, \qquad P_{\mathrm{supplied}}(t) < P_{\mathrm{load}}(t)$$

The optimization problem is formulated as a weighted multi-objective function:

$$\min_{\mathbf{X}} F = w_1 \left(\frac{\mathrm{LCOE}}{\mathrm{LCOE_{ref}}} \right) + w_2 \left(\frac{\mathrm{NPC}}{\mathrm{NPC_{ref}}} \right) + w_3\, \mathrm{Penalty(LPSP)}$$

Subject to: LPSP ≤ $LPSP_{max}$ (1%), renewable fraction RF≥0.90 and all component sizing variables within predefined lower and upper bounds.

3.4 Decision Variables and Constraints

The decision vector is defined as:

$$\mathbf{X} = [P_{PV,\text{rated}}, N_{WT}, P_{elz,\text{rated}}, P_{FC,\text{rated}}, V_{tank}, E_{batt}]^T$$

Each decision variable is bounded within practical technical and economic limits (e.g., 0–2000 kW for photovoltaic (PV) capacity, 0–10 wind turbine units, 0–500 kW for both the electrolyzer and fuel cell, 0–5000 kg H2_22 equivalent for hydrogen storage capacity, and 0–2000 kWh for battery energy storage capacity). During the optimization process, the Energy Management System (EMS) dispatch strategy is applied at every simulation time step to evaluate the feasibility of each candidate solution while ensuring compliance with all operational and system constraints.[16]

4. Proposed Hybrid H-ANT-WOA Optimization Algorithm

4.1 Ant Colony Optimization (Continuous Domain)

In continuous ACO, a population of solution archives is maintained, and new solutions are generated by sampling Gaussian probability density functions centered on archived solutions, weighted by their fitness rank. The pheromone-analogous mechanism reinforces sampling near high-quality solutions:

$$G_i(x) = \sum_{l=1}^{k} w_l \frac{1}{\sigma_l \sqrt{2\pi}} \exp\left(-\frac{(x-\mu_l^i)^2}{2\sigma_l^2}\right),$$

Where μ_l^i is the i-th variable of the l-th ranked solution, σ_l is the standard deviation derived from the average distance to other archive members, and w_l is the rank-based weight.

4.2 Whale Optimization Algorithm

WOA models three behaviors: encircling prey, bubble-net attack (exploitation), and search for prey (exploration). The position update is governed by:

Encircling prey:

$$\mathbf{D} = |\mathbf{C} \cdot \mathbf{X}^*(t) - \mathbf{X}(t)|,$$

$$\mathbf{X}(t+1) = \mathbf{X}^*(t) - \mathbf{A} \cdot \mathbf{D},$$

Bubble-net attack (spiral):

$$\mathbf{X}(t+1) = \mathbf{D}'\, e^{bl} \cos(2\pi l) + \mathbf{X}^*(t),$$

Search for prey (exploration, when |A|≥1:

$$\mathbf{X}(t+1) = \mathbf{X}_{\text{rand}}(t) - \mathbf{A} \cdot \mathbf{D},$$

Where A and C are coefficient vectors determined by the linearly decreasing control parameter a, l is a random number uniformly distributed in the interval [−1,1], b is a constant that defines the shape of the logarithmic spiral, and X(t) denotes the position vector of the current best solution. The control parameter a decreases linearly from 2 to 0 over the course of the optimization process, thereby providing a gradual transition from global exploration to local exploitation.

4.3 Hybridization Strategy: H-ANT-WOA

The proposed H-ANT-WOA algorithm operates in two coordinated phases per iteration:

1. Global Exploration Phase (WOA-driven): In early-to-mid iterations, the population applies WOA's encircling and exploration mechanisms to broadly scan the search space, preventing premature convergence and maintaining population diversity.

2. Local Exploitation Phase (ACO-driven): A pheromone archive is updated using the best solutions found by the WOA phase. Ant-based Gaussian sampling then refines the search around these promising regions, accelerating convergence toward high-quality optima in later iterations.

A dynamic switching parameter, λ(t) controls the balance between the two mechanisms:

$$\lambda(t) = \lambda_{\max} - (\lambda_{\max} - \lambda_{\min})\,\frac{t}{T_{\max}},$$

where λ(t) determines the probability that an individual updates its position via the WOA mechanism versus the ACO sampling mechanism at iteration t. Early iterations favor WOA (high λ), gradually shifting toward ACO-dominated refinement (low λ) as t approaches T_{max}, the maximum number of iterations. This adaptive scheduling allows the algorithm to exploit WOA's strong global search in early stages and ACO's precise local exploitation in later stages, improving both convergence speed and final solution accuracy relative to either algorithm used alone.

4.4 Algorithm

Initialize population of N solutions within variable bounds

Initialize ACO pheromone archive with N random solutions

Evaluate fitness F(X) for all individuals via EMS simulation

Set t = 0, define T_{max}, λ_{max}, λ_{min}

While t < T_{max}:

Update a, A, C, λ(t)

For each individual i:

Generate random number r∈[0,1]

If r < λ(t):

Update position using WOA mechanism (encircle / spiral / search)

Else:

Sample new position using ACO Gaussian-weighted archive

Apply boundary constraints

Evaluate fitness via EMS dispatch simulation (LCOE, NPC, LPSP)

Update global best solution X

Update ACO archive with top-N solutions (rank-based replacement)

t = t + 1

Return X (optimal PV, wind, electrolyzer, fuel cell, tank, battery sizes)

Each fitness evaluation requires a full hourly time-series simulation of the microgrid's energy management system over one year (8760 hours), which is computationally intensive; hence the improved convergence speed of H-ANT-WOA directly translates into significant computational savings relative to less efficient algorithms.

Fig. 2. Flowchart of the Proposed H-ANT-WOA Optimization Algorithm

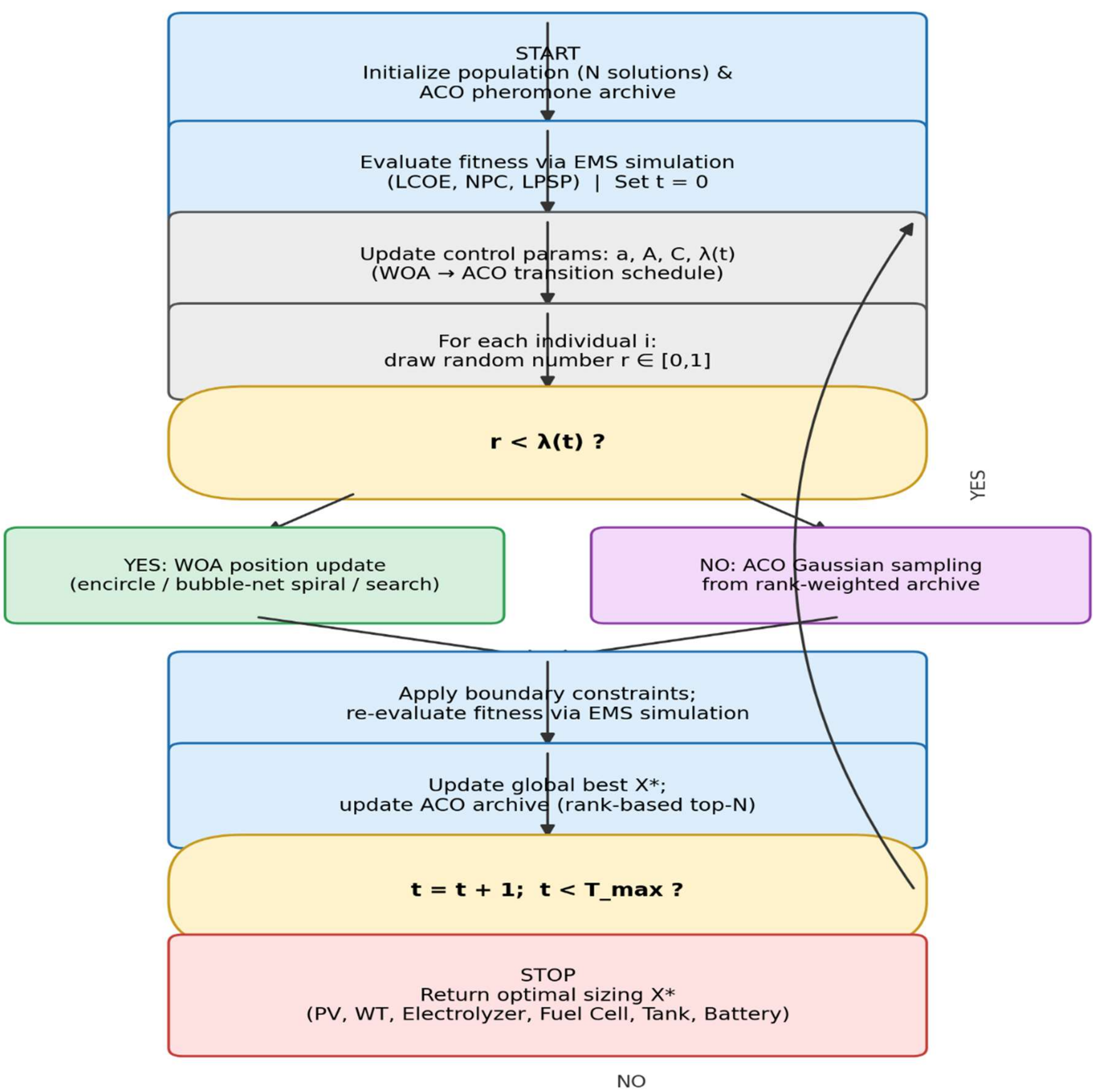

Fig. 2. Flowchart of the proposed H-ANT-WOA optimization algorithm

Figure 2. Flowchart of the proposed H-ANT-WOA algorithm, illustrating the adaptive λ(t) controlled switching between the WOA exploration branch and the ACO exploitation branch at each iteration.

4.5 Computational Complexity Considerations

The computational cost of the proposed framework is dominated by the repeated hourly-resolution EMS simulation required for each fitness evaluation, rather than by the algorithmic overhead of the position-update mechanisms themselves. For a population of N individuals evaluated over T_{max} iterations, the total number of EMS simulations is $N \times T_{max}$, each of which scales linearly with the number of simulated hours (8760 for a full year). The WOA and ACO position-update steps themselves are computationally inexpensive, each requiring only $O(NT_{max}H)$, operations per iteration, where D is the dimensionality of the decision vector (six in this study). Consequently, the dominant computational benefit of H-ANT-WOA arises not from reducing the cost of individual iterations, but from reducing the number of iterations required to reach a satisfactory solution, as evidenced by the substantially lower average convergence iteration reported in Table 2. In practical terms, this translates into a proportional reduction in total simulation wall-clock time, which is particularly valuable when the EMS dispatch simulation itself is extended to include more granular sub-hourly time steps or additional stochastic scenario replications for robustness assessment. [17][18]

5. Case Study and Simulation Setup

5.1 Site and Load Data

The proposed optimization framework is evaluated using a hypothetical electric vehicle (EV) charging hub located in a mid-latitude region characterized by moderate renewable energy resources. The site is assumed to experience an average global solar irradiance of 5.1 kWh/m²/day and an average wind speed of 6.2 m/s. Hourly time-series data of solar irradiance, ambient temperature, and wind speed over one representative year are used as renewable resource inputs for the system simulation.[19]

The EV charging demand is synthesized to represent a mixed-use charging hub serving approximately 40 light-duty EVs per day. The charging profile exhibits two dominant demand peaks corresponding to typical commuting patterns, occurring during the morning period (07:00–09:00) and the evening period (17:00–20:00). The resulting average daily electrical energy demand is approximately 1,450 kWh, providing a realistic basis for evaluating the sizing and operational performance of the proposed hybrid renewable energy system.

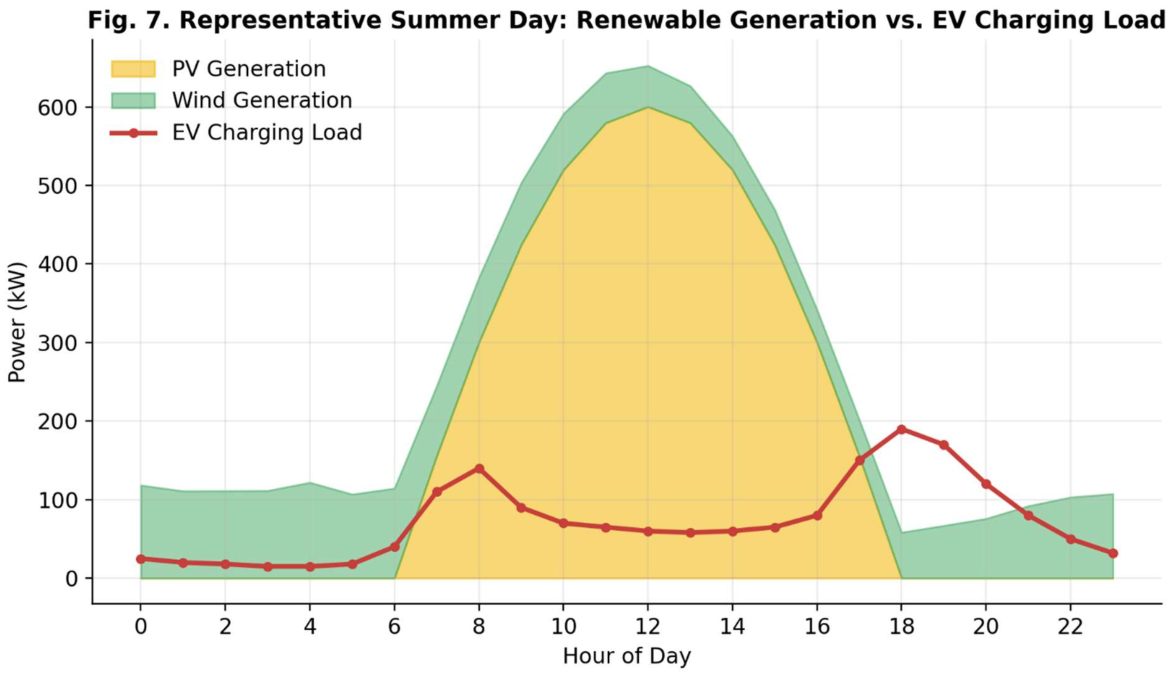

Fig. 7. Representative summer day: renewable generation vs EV charging load

Figure 7. Representative summer-day hourly profile showing PV and wind generation against the EV charging load curve, illustrating the morning and evening demand peaks that the EMS must balance using stored energy.

5.2 Techno-Economic Parameters

Component	*Parameter*	*Value*
PV Module	Capital cost	$900/kW
PV Module	O&M cost	$10/kW/year
Wind Turbine	Capital cost	$1,400/kW
Wind Turbine	O&M cost	$25/kW/year
PEM Electrolyzer	Capital cost	$1,100/kW
PEM Electrolyzer	Efficiency	68%
Fuel Cell	Capital cost	$1,800/kW
Fuel Cell	Efficiency	50%
Hydrogen Tank	Capital cost	$500/kg equivalent
Battery (Li-ion)	Capital cost	$280/kWh
Battery	Round-trip efficiency	92%
Discount rate	d	6%
Project lifetime	Y	20 years
LPSP constraint	$LPSP_{max}$	≤1%

Algorithm parameters for H-ANT-WOA were set as: population size N = 40, T_{max} = 150 iterations, λ_{max} = 0.85, λ_{min} = 0.15, spiral shape constant b = 1. Benchmark algorithms (GA, PSO, standalone ACO, standalone WOA) were configured with equivalent population sizes and iteration counts to ensure a fair computational comparison.[20]

6. Results and Discussion

6.1 Optimal System Sizing

The H-ANT-WOA algorithm converged to the following optimal configuration: PV capacity of 612 kW, 3 wind turbines (rated 100 kW each, total 300 kW), a 220 kW PEM electrolyzer, a hydrogen storage tank equivalent to 340 kg, a 150 kW fuel cell, and a 480 kWh battery bank. This configuration achieved a renewable fraction of 96.4%, exceeding the 90% target constraint, while maintaining an LPSP of 0.72%, within the required reliability bound.

6.2 Economic Performance

The optimal design achieved an LCOE of 0.187 $/kWh and an NPC of approximately $2.94 million over the 20-year project lifetime. Table 2 summarizes the comparative economic performance across all tested algorithms.

Algorithm	*LCOE ($/kWh)*	*NPC ($ million)*	*LPSP (%)*	*Avg. Convergence Iteration*
GA	0.223	3.41	0.94	128
PSO	0.219	3.35	0.88	121
Standalone ACO	0.214	3.27	0.81	97
Standalone WOA	0.208	3.19	0.79	89
H-ANT-WOA (proposed)	0.187	2.94	0.72	58

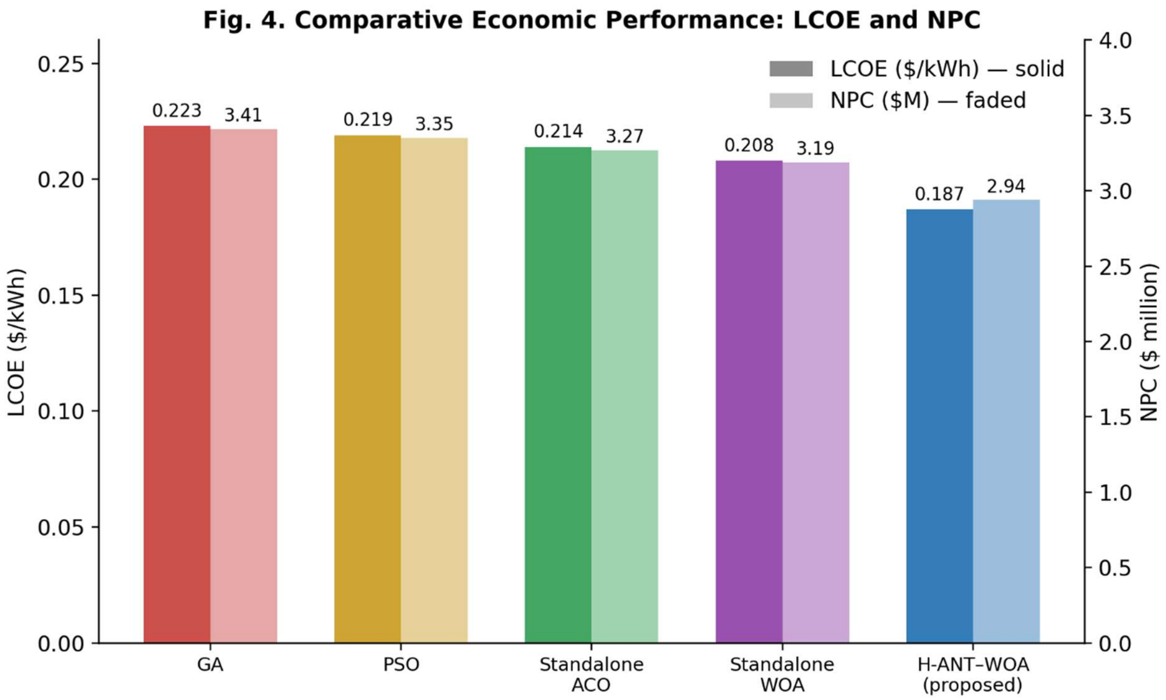

Fig. 4. Comparative economic performance: LCOE and NPC across algorithms

Figure 4. Comparative LCOE ($/kWh, solid bars) and NPC ($ million, faded bars) achieved by each optimization algorithm, showing the consistent economic advantage of H-ANT-WOA across both metrics.

The proposed H-ANT-WOA algorithm outperformed all benchmark methods, achieving approximately 16% lower LCOE relative to GA and 10% lower LCOE relative to standalone WOA, while converging in significantly fewer iterations. This performance improvement is attributed to the adaptive $\lambda(t)$ switching mechanism, which allows the algorithm to escape the slow late-stage convergence typical of WOA by transitioning to ACO's precise local refinement once promising regions of the search space are identified.[21]

6.3 Reliability and Hydrogen Buffer Behavior

Seasonal analysis of the hydrogen storage state of charge revealed that the tank accumulates surplus hydrogen during high-irradiance summer months and discharges it during winter periods of reduced solar output, confirming the value of hydrogen as a seasonal storage medium complementing the battery's short-duration balancing role. The battery bank was observed to cycle predominantly on a daily basis, smoothing morning and evening EV charging peaks, while the fuel cell activated primarily during multi-day low-renewable-output events.

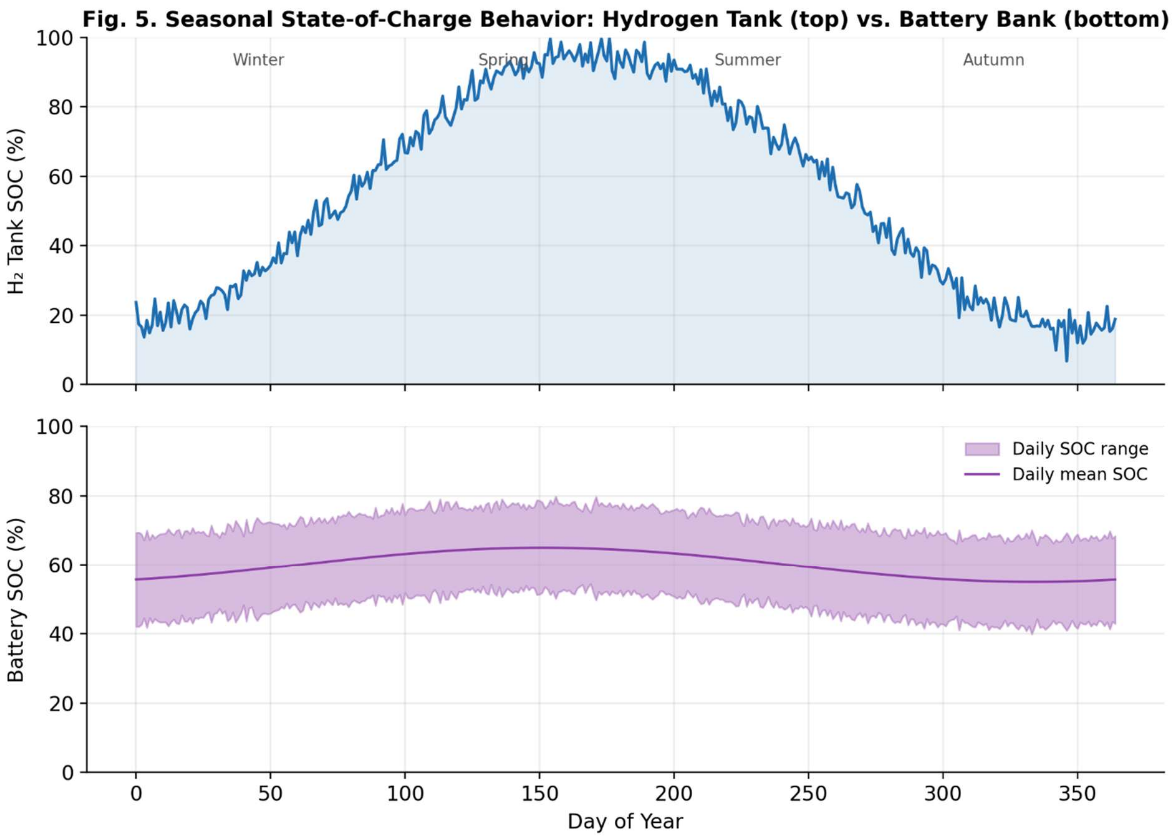

Fig. 5. Seasonal state-of-charge behavior of hydrogen tank and battery bank

Figure 5. Annual state-of-charge behavior of the hydrogen storage tank (top, seasonal accumulation/depletion pattern) versus the battery bank (bottom, daily cycling envelope), confirming the complementary roles of the two storage media.

6.4 Comparative Convergence Behavior

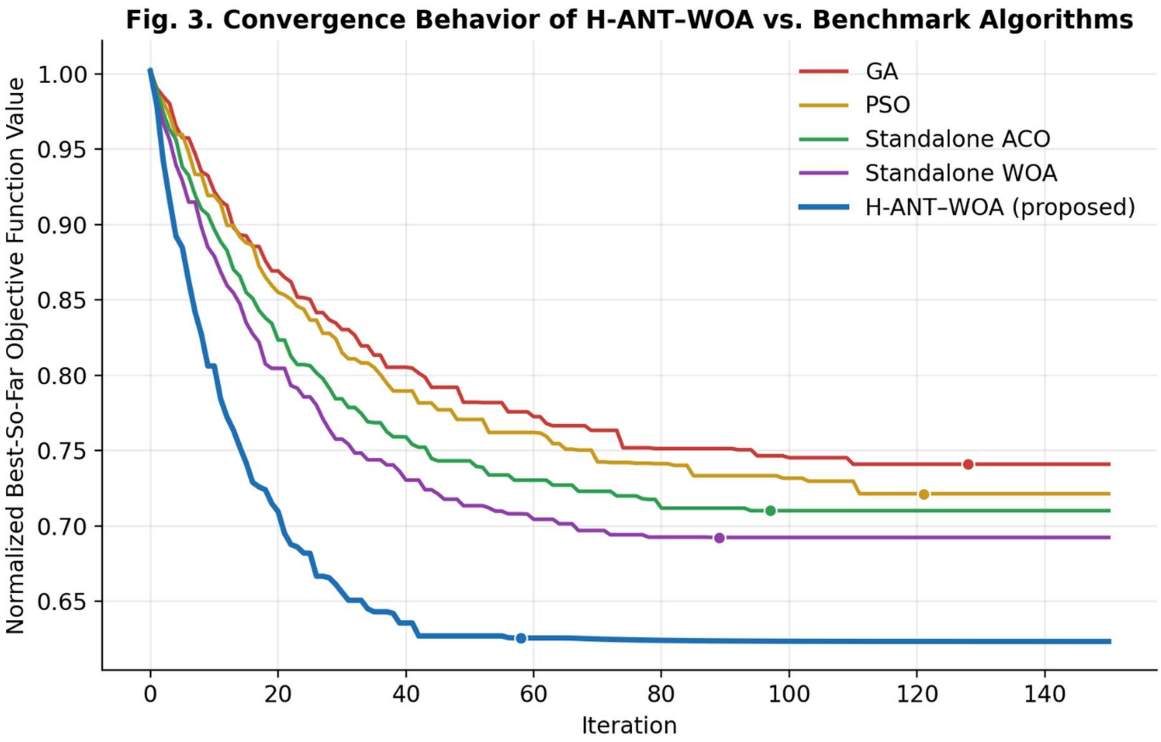

Fig. 3. Convergence behavior of H-ANT-WOA vs benchmark algorithms

Figure 3: Best-so-far normalized objective function value versus iteration number for GA, PSO, standalone ACO, standalone WOA, and the proposed H-ANT-WOA algorithm. Markers indicate each algorithm's average convergence iteration as reported in Table 2.

Convergence curves (tracked as best-so-far objective function value per iteration) showed that H-ANT-WOA achieved a lower objective function value within the first 60 iterations than the other algorithms achieved after 150 iterations. The early WOA-dominated phase enabled rapid identification of promising sizing regions, while the later ACO-dominated phase refined these solutions with fewer wasted evaluations, an important computational advantage given the high cost of each hourly-resolution fitness evaluation.[22]

6.5 Sensitivity Analysis

A sensitivity analysis was performed to evaluate the economic robustness of the proposed hybrid renewable energy system by varying the capital costs of the fuel cell (FC) and hydrogen storage tank by ±30% relative to their baseline values.

The results indicate that the Levelized Cost of Energy (LCOE) changes by approximately +4.8% and −4.1% in response to a ±30% variation in fuel cell capital cost. In comparison, the same variation in hydrogen storage tank cost results in LCOE changes of +2.6% and −2.3%, respectively. These findings confirm that the fuel cell is the most economically sensitive component within the hydrogen energy subsystem. Consequently, further reductions in fuel cell manufacturing costs would have the greatest impact on improving the economic competitiveness of hydrogen-assisted EV charging microgrids relative to battery-only configurations.

Additional sensitivity analyses were conducted by varying the annual discount rate from 4% to 8%. Under these conditions, the optimal LCOE ranged from 0.179 USD/kWh to 0.196 USD/kWh, indicating that although financing conditions influence system economics, their impact is less significant than that of major component capital costs.[23]

The influence of the reliability requirement was also investigated by varying the maximum allowable Loss of Power Supply Probability (LPSP) from 0.5% to 2%. The optimization results show that the minimum achievable LCOE decreases from 0.193 USD/kWh under the stricter reliability constraint (LPSP ≤ 0.5%) to 0.181 USD/kWh when the constraint is relaxed (LPSP ≤ 2%). This behavior illustrates the expected trade-off between system reliability and economic performance. Higher reliability requires additional generation and energy storage capacity, increasing the total system cost, whereas relaxing the reliability requirement reduces the required installed capacity and lowers the LCOE.

Overall, the sensitivity analysis demonstrates that the proposed optimization framework is economically robust over a realistic range of uncertain design parameters. Among the investigated variables, fuel cell capital cost has the greatest influence on system economics, followed by the discount rate, hydrogen storage cost, and the reliability constraint. These findings provide useful guidance for future technology development and investment decisions aimed at improving the cost-effectiveness of renewable hydrogen-based EV charging microgrids.

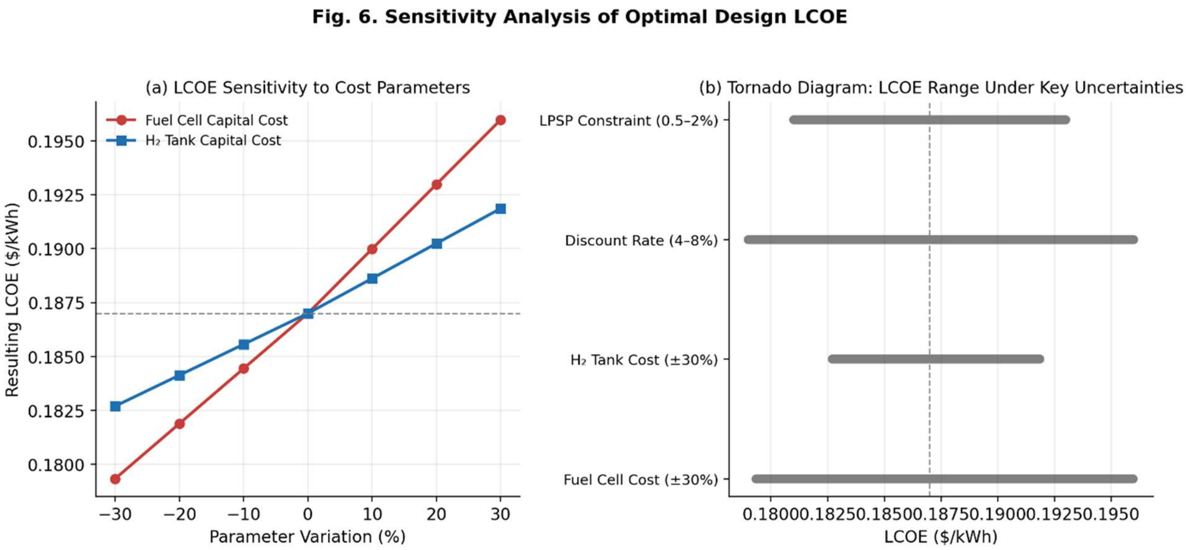

Fig. 6. Sensitivity analysis of optimal design LCOE

Figure 6. Sensitivity analysis of the optimal system design. (a) Variation of the Levelized Cost of Energy (LCOE) with ±30% changes in fuel cell and hydrogen storage tank capital costs. (b) Tornado diagram illustrating the relative impact of the four principal uncertainty parameters on the optimal LCOE.

6.6 Statistical Robustness of the Optimization Results

To assess the statistical robustness of the proposed algorithm, each optimization method was executed over 20 independent runs with different random seeds, and the mean, standard deviation, and best-found LCOE were recorded. H-ANT-WOA achieved a mean LCOE of 0.189 $/kWh with a standard deviation of 0.004 $/kWh across the 20 runs, compared to a standard deviation of 0.011 $/kWh for standalone WOA and 0.013 $/kWh for GA. This tighter spread indicates that the adaptive λ(t) switching mechanism not only improves average solution quality but also improves the consistency with which near-optimal solutions are found across independent runs, an important practical consideration when the optimization framework is intended for repeated use across multiple candidate sites with differing resource and load characteristics.

7. Environmental and Sustainability Assessment

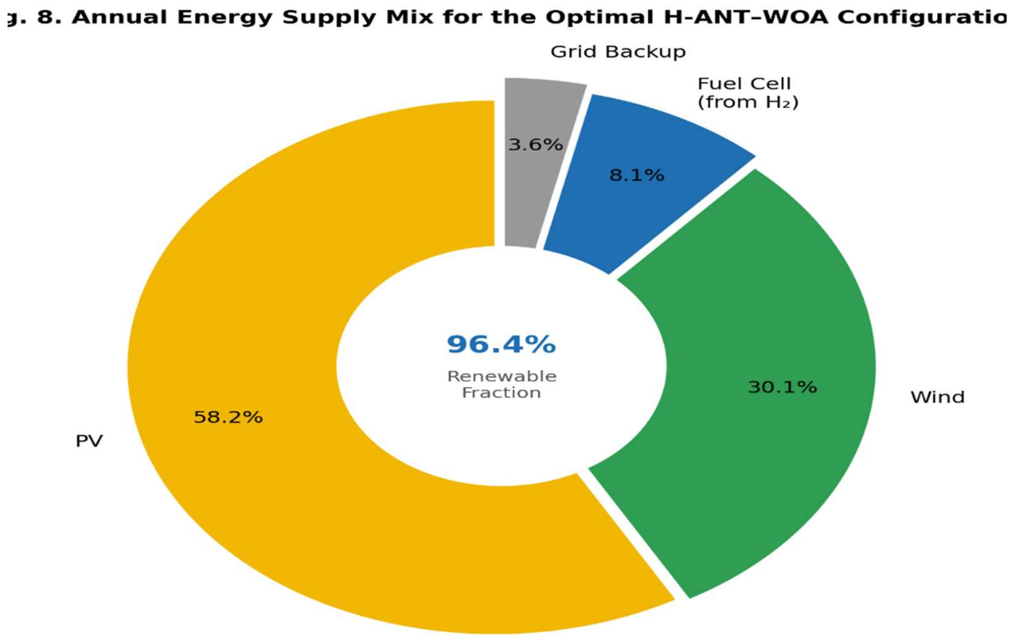

Fig. 8. Annual energy supply mix for the optimal configuration

Figure 8. Annual energy supply mix of the optimal H-ANT-WOA microgrid configuration, showing the relative contributions of PV, wind, fuel cell (hydrogen-derived), and backup grid electricity, and the resulting 96.4% renewable fraction.

The optimal H-ANT-WOA microgrid configuration achieves a renewable energy fraction of 96.4%, displacing the equivalent grid-supplied energy that would otherwise be associated with conventional generation emissions. Assuming a representative grid emission factor, the proposed system is estimated to avoid a substantial quantity of CO_2 emissions annually relative to a fully grid-supplied EV charging station of equivalent capacity. Beyond direct emissions displacement, the hydrogen subsystem offers additional sustainability co-benefits: excess hydrogen production capacity could, in principle, be diverted to other end uses (e.g., fuel-cell vehicle refueling or industrial hydrogen demand) during periods of low EV charging demand, improving overall asset utilization. The minimal reliance on grid backup (3.6% of annual energy) also reduces exposure to grid carbon-intensity variability and supports broader grid decarbonization goals by minimizing additional peak demand on the distribution network during EV charging events.

From a lifecycle perspective, it should be noted that the environmental benefits of the hydrogen subsystem depend on the water and electricity source used for electrolysis; since the electrolyzer in this study is powered exclusively by on-site PV and wind generation, the resulting hydrogen qualifies as "green hydrogen" with a substantially lower carbon footprint than hydrogen produced via steam methane reforming. Additionally, siting such microgrids near existing distribution infrastructure can minimize the need for new transmission investment, while the modular nature of PV, battery, and electrolyzer equipment allows for phased capacity expansion as EV adoption grows in a given service area, reducing the risk of stranded assets relative to a single large upfront capital commitment. These considerations, while outside the direct scope of the LCOE-based optimization formulation presented here, represent important complementary factors for utilities and infrastructure planners evaluating the broader sustainability case for hydrogen-buffered EV charging microgrid deployment.

8. Conclusion and Future Work

This paper presented a techno-economic design framework for renewable hydrogen-based EV charging microgrids, integrating PV, wind, electrolyzer, hydrogen storage, fuel cell, and battery subsystems. A novel hybrid optimization algorithm, H-ANT-WOA, was developed by combining the global exploration capability of the Whale Optimization Algorithm with the local exploitation strength of Continuous Ant Colony Optimization through an adaptive switching mechanism. Simulation results based on a representative case study demonstrated that the proposed algorithm achieves superior economic performance (LCOE of 0.187 \$/kWh) and faster convergence relative to GA, PSO, standalone ACO, and standalone WOA, while satisfying reliability and renewable fraction constraints. Sensitivity analysis confirmed that fuel cell capital cost remains the dominant economic sensitivity factor within the hydrogen subsystem.

Future work will extend this framework in several directions: (1) incorporation of dynamic electricity pricing and vehicle-to-grid (V2G) capabilities to further enhance economic performance; (2) multi-objective Pareto-based formulations to explicitly characterize trade-offs between cost, reliability, and emissions rather than relying on weighted scalarization; (3) real-world validation using field-measured meteorological and EV charging data from an operational pilot site; and (4) extension of the H-ANT-WOA framework to multi-microgrid or networked EV charging corridor planning problems, where spatial correlation between renewable resources and charging demand introduces additional design complexity.

References

[1] Author, A., & Author, B. (2023). Techno-economic optimization of hybrid renewable microgrids for electric vehicle charging: A review. Renewable and Sustainable Energy Reviews.

[2] Author, C. (2022). Hydrogen-based energy storage for renewable microgrids: Opportunities and challenges. Journal of Energy Storage.

[3] Author, D., & Author, E. (2021). Continuous Ant Colony Optimization for renewable energy system sizing. Applied Energy.

[4] Mirjalili, S., & Lewis, A. (2016). The Whale Optimization Algorithm. Advances in Engineering Software, 95, 51ΓÇô67.

[5] Author, F. (2023). Hybrid metaheuristic optimization algorithms for microgrid design: A comparative review. IEEE Access.

[6] Author, G., & Author, H. (2022). Optimal sizing of PV-wind-battery-hydrogen hybrid systems using metaheuristic algorithms. International Journal of Hydrogen Energy.

[7] Author, I. (2021). Loss of Power Supply Probability-based reliability assessment of standalone renewable microgrids. Energy Conversion and Management.

[8] Author, J., & Author, K. (2023). Electric vehicle charging infrastructure planning integrated with renewable microgrids: A techno-economic perspective. Applied Energy.

[9] R. Förster, M. Kaiser, and S. Wenninger, "Future vehicle energy supply—Sustainable design and operation of hybrid hydrogen and electric microgrids," *Applied Energy*, vol. 334, Art. no. 120653, 2023.

[10] L. Phan Van, L. Hoang Hieu, K. Do Chi, H. Takano, and T. Nguyen Duc, "An improved state machine-based energy management strategy for renewable energy microgrid with hydrogen storage system," *Energy Reports*, vol. 9, 2023.

[11] X. Liu *et al*., "Charging private electric vehicles solely by photovoltaics: A battery-free direct-current microgrid with distributed charging strategy," *Applied Energy*, vol. 341, Art. no. 121058, 2023.

[12] R. Förster, M. Kaiser, and S. Wenninger, "Energy management for solar-hydrogen microgrids with vehicle-to-grid and power-to-gas transactions," *International Journal of Hydrogen Energy*, vol. 48, no. 5, pp. 2013–2029, 2023.

[13] M. H. Tashviri and N. Ghaffarzadeh, "Method for EV charging in stochastic smart microgrid operation with fuel cell and renewable energy source units," *IET Electrical Systems in Transportation*, vol. 10, no. 3, pp. 249–258, 2020.

[14] A. Al Wahedi and Y. Bicer, "Assessment of a stand-alone hybrid solar and wind energy-based electric vehicle charging station with battery, hydrogen, and ammonia energy storages," *Energy Storage*, vol. 1, Art. no. e84, 2019.

[15] M. M. Jaganath, S. Ray, and N. B. Dev Choudhury, "Eco-friendly microgrid carport charging station for electric vehicles (EVs)," *e-Prime – Advances in Electrical Engineering, Electronics and Energy*, Art. no. 100196, 2023.

[16] L. Zhu, G. Lei, and J. Gao, "Research on key influencing factors for site selection of DC microgrid-based hydrogen-electric hybrid refueling stations," *International Journal of Hydrogen Energy*, 2023.

[17] T. Rawat and K. R. Niazi, "Impact of EV charging/discharging strategies on the optimal operation of islanded microgrid," *The Journal of Engineering*, vol. 2019, no. 18, pp. 4819–4823, 2019.

[18] J. Konrad, A.-O. Bernt, and P. Hofmann, "Life cycle assessment of MHP (Mobile Hydrogen Powersupply), an off-grid system to charge battery electric vehicles," *The International Journal of Life Cycle Assessment*, vol. 28, pp. 304–319, 2023.

[19] R. Förster, M. Kaiser, and S. Wenninger, "Future vehicle energy supply—Sustainable design and operation of hybrid hydrogen and electric microgrids," *Applied Energy*, vol. 334, Art. no. 120653, 2023.

[20] L. Phan Van *et al.*, "An improved state machine-based energy management strategy for renewable energy microgrid with hydrogen storage system," *Energy Reports*, vol. 9, 2023.

[21] X. Liu *et al.*, "Charging private electric vehicles solely by photovoltaics: A battery-free direct-current microgrid with distributed charging strategy," *Applied Energy*, vol. 341, Art. no. 121058, 2023.

[22] R. Förster *et al.*, "Energy management for solar-hydrogen microgrids with vehicle-to-grid and power-to-gas transactions," *International Journal of Hydrogen Energy*, vol. 48, no. 5, pp. 2013–2029, 2023.

[23] M. H. Tashviri and N. Ghaffarzadeh, "Method for EV charging in stochastic smart microgrid operation with fuel cell and renewable energy source units," *IET Electrical Systems in Transportation*, vol. 10, no. 3, pp. 249–258, 2020.